Results in Physics 24 (2021) 104134

Contents lists available at ScienceDirect

Results in Physics

journal homepage: www.elsevier.com/locate/rinp

Tunable acoustic hooks from Janus cylinder

Sergio Castiñeira-Ibañez, Daniel Tarrazó-Serrano, Antonio Uris, Constanza Rubio *

Centro de Tecnologías Físicas: Acústica, Materiales y Astrofísica, Universitat Politècnica de València, Camino de Vera s/n, 46022 Valencia, Spain

ARTICLE INFO

Keywords:
Acoustic hook
Janus cylinder
Acoustojet
Sonic crystal

ABSTRACT

In this paper we present a new way to obtain tunable acoustic hooks. The breaking of the symmetry of the material composition is used for the generation of acoustic hooks from Janus cylinders. This fact is possible by using sonic crystals to vary the refractive index of two half-cylinders. The study has been carried out numerically, using the Finite Element Method. By changing the contrast of refractive indexes between the two half-cylinders or by rotating the Janus cylinder, acoustic hooks can be obtained that can be tunable with bending angle ranging from 1° to 21°. Full Width at Half-Maximum can be obtained with values close to the diffraction limit. This structure provides an efficient method to precisely tune the acoustic hook depending on it use.

Introduction

The idea that a wave, of whatever type, propagates in a straight line in a homogeneous medium has been known since ancient times. Of the different phenomena that they can present, wave beam bending has attracted interest from researchers and has been under investigation since Siviloglou et al. [1,2] proposed and experimentally observed in 2007, the possibility of an electromagnetic wave propagating along a curved path. This exotic behavior arises from quantum mechanics: a beam can propagate in a curved path if the quantum wave function follows an Airy profile [3]. An overview in the field of Airy beams can be found in Ref. [4].

In 2018, a near-field curved optical beam [5] was presented whose origin is different from those of Airy beams. This new curved optical beam was named "photonic hook", and was observed experimentally in the Terahertz range in 2019 [6]. This phenomenon has also been demonstrated for surface plasmon waves [7]. The photonic hook is obtained when a plane wave hits an asymmetric dielectric particle. Due to the phase velocity difference and wave interference between the upper and lower parts of the particle, a curved light beam forms near the particle shadow surface.

The concept of photonic hook has recently been extended, to other type of waves such as acoustic waves, by Rubio et al. [8]. They first reported both experimental and simulated observation of a new type of curved acoustic beam, which they called "acoustic hook". This curved acoustic beam was generated using a trapezoidal-rectangular prism Rexolite® particle immersed in water, which is incident on an ultrasonic flat wave at the frequency of 250 kHz. As in the case of electromagnetic waves, the acoustic hook is produced by the breakdown of the structural symmetry of the particle. Other method could be used to break the particle's symmetry. Gu and Geints et al. proposed refractive index contrast modification between parts of the particle [9,10] using two different materials to build the particle.

In this paper, we demonstrate by numerical simulation that acoustic hooks can be generated from a Rexolite® cylinder. Varying the speed of sound propagation of each half of the cylinder result on each half of the cylinder has a different refractive index. These types of particles are the so-called the Janus cylinder. To achieve a contrast of refractive indices in the cylinder, a Sonic Crystal (SC) will be used in one of the halves. The influence on the bending of the refractive index contrast between the two halves will be analyzed. The variation of the refractive index will be carried out by modifying the filling factor of the SC, with which the tunability of these acoustic hooks will be achieved.

Numerical modelling

Numerical simulations were conducted using a commercial software COMSOL Multiphysics© using Finite Elements Method to investigate the acoustic field distribution inside and outside the particle. To reduce the computational cost and take advantage of the limit and initial conditions of the problem, a two-dimensional model has been used. This is possible given that the height of the cylinder is considered enough large compared to its transverse dimensions, in addition to analyzing the pressure field in the vicinity of the cylinder surface (Fig. 1). Fig. 2 shows the details of the implemented FEM model: a cylinder of material (Rexolite®) is introduced into a medium (water). Therefore, two

* Corresponding author.
E-mail address: crubiom@fis.upv.es (C. Rubio).

https://doi.org/10.1016/j.rinp.2021.104134
Received 16 September 2020; Received in revised form 24 March 2021; Accepted 26 March 2021
Available online 4 April 2021

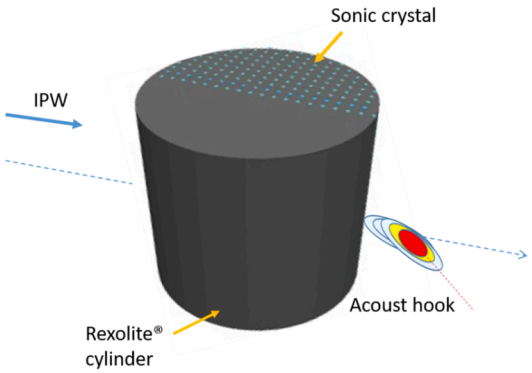

Fig. 1. A Rexolite® cylinder in which it is divided into two halves with different refractive index generates an acoustic hook. The incident wave is considered an Incident Plane Wave (IPW).

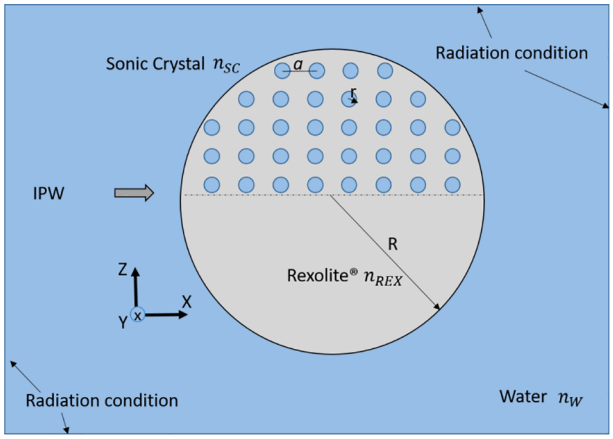

Fig. 2. Scheme of the geometry and boundary conditions of the implemented FEM model. n_W n_{SC}, and n_{REX} are the refractive indices of water, SC and Rexolite®, respectively. The Rexolite® cylinder is divided into two halves with different refractive index, the upper part n_{SC} and the lower part n_{REX}.

perfectly coupled physical modules were used to obtain the solution. To achieve a perfectly matched system, the contours of the cylinder, as well as the contours of SC within the cylinder, are included in the multi-physics module so that the interaction of solid structure is achieved, considering that the Rexolite® cylinders had two sound propagation speeds (longitudinal and shear). The solid mechanical modulus resolved the solid-structure interaction in the cylinder that was implemented as an isotropic linear elastic material, using three Rexolite® physical parameters: longitudinal wave velocity ($c_l = 2337$ m/s), shear wave velocity ($c_s = 1157$ m/s) and density ($\rho_{REX} = 1049$ kg/m^3). The acoustic module contained the solution for the host domain (water) considering the speed of sound ($c = 1500$ m/s) and density ($\rho = 1000$ kg/m^3). The background pressure field was selected to emulate the plane wave incident. To emulate an infinite medium and avoid reflections on the model walls, the edges of the host were defined as radiation contours. In this way, Sommerfeld condition is obtained. The mesh was defined as a triangular typology. To avoid numerical dispersion, the maximum size of the mesh element was $\lambda/10$.

Results

The existence of an intense acoustic field located on the shadow surface of a particle, also called an acoustic jet (AJ), is known when an acoustic wave hits it [11,12,13]. If the particle is of a homogeneous material, the AJ is symmetric about the axis in the direction of propagation. However, the acoustic intensity and the Full Width at Half Maximum (FWHM) of the AJ depend on the material and the particle size. FWHM being the distance between the two points adjacent to the maximum value at which the normalized acoustic intensity reaches the half its maximum value. The effect of Rexolite® cylinder size on the normalized acoustic intensity I_{max}/I_{inc} (where I_{max} is the maximum AJ intensity and I_{inc} is the incident intensity) and on the FWHM was studied in a range of radius $R = 3\lambda - 6\lambda$, where λ is the average wavelength of the host, which was water. The incident plane wave of $f = 250$ kHz propagates along the X direction. The values of I_{max}/I_{inc} and FWHM are presented in Table 1. It is observed that the maximum value of I_{max}/I_{inc} is obtained for a radius of cylinder of $R = 4.75\lambda$, being its FWHM $= 0.531\ \lambda$, which can be considered subwavelength. That's why the cylinder radius was established as 4.75λ, value obtained by parametric resolution of the numerical model. Fig. 3 shows the distribution of the acoustic intensity I_{max}/I_{inc} in XZ planes around and inside the Rexolite® cylinder with a radius R equal to 4.75λ. In this case, an acoustojet with a symmetrical pattern is observed.

Once the radius of the cylinder was selected, it was replaced by a Janus cylinder. To achieve this, the upper-half cylinder was drilled to create a SC (see Fig. 4), while the lower-half cylinder was not modified. As the cylinder was immersed in water, the inner of the holes was also

Table 1
Numerical parameter results for different Rexolite® cylinder radius, R.

R/λ	I_{max}/I_{inc}	FWHM/λ
3.00	4.13	0.43
3.50	3.21	0.73
4.00	3.46	0.58
4.50	4.67	0.47
4.75	4.91	0.53
5.00	3.85	0.46
5.50	4.19	0.58
6.00	4.05	0.52

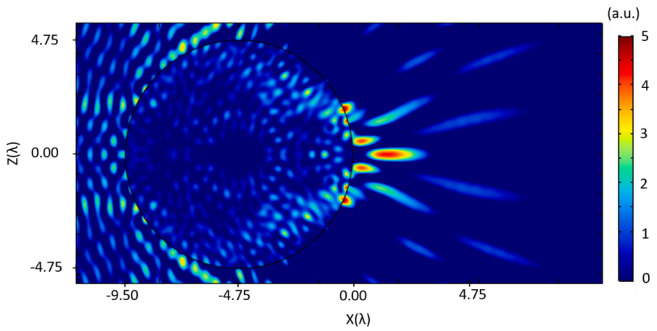

Fig. 3. Acoustic intensity distribution (I_{max}/I_{inc}) (arbitrary units) for a homogeneous Rexolite® cylinder of radius $R = 4.75\lambda$.

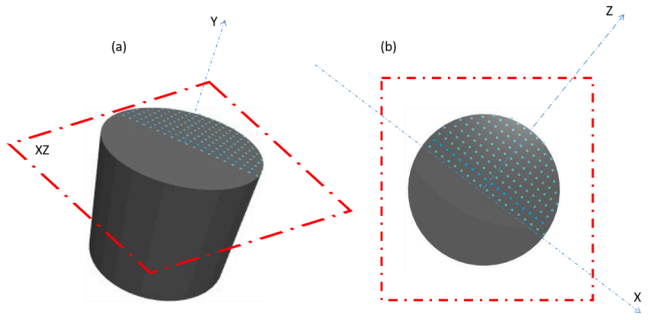

Fig. 4. (a) 3D cylinder (b) 2D sectional view (The cross section of the cylinder that is located in the XZ plane is analyzed).

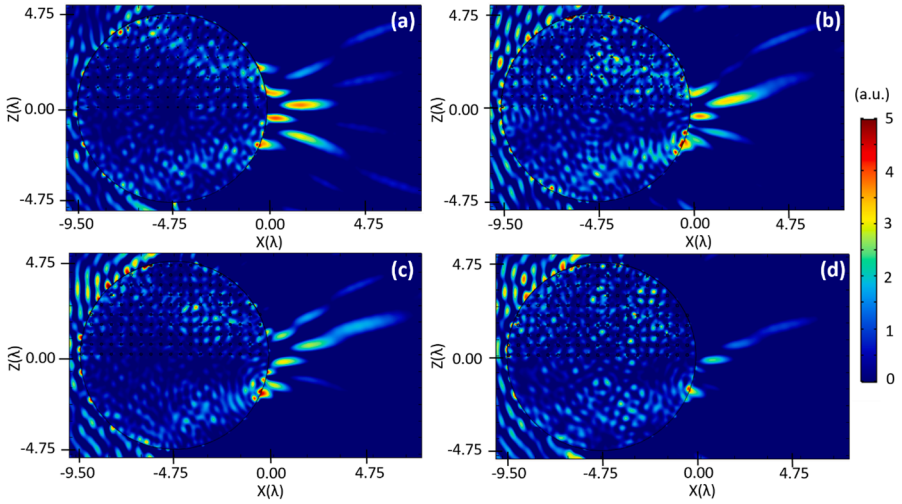

Fig. 5. Distribution of the normalized acoustic intensity I_{max}/I_{inc} in XZ planes around and inside the Janus cylinder with a radius R equal to 4.75λ and with a SC with a = 3 mm and different hole radii on the upper-half cylinder: (a) r = 0.20 mm or r = 0.033λ, (b) r = 0.30 mm or r = 0.050λ, (c) r = 0.35 mm or r = 0.058λ, (d) r = 0.40 mm or r = 0.066λ.

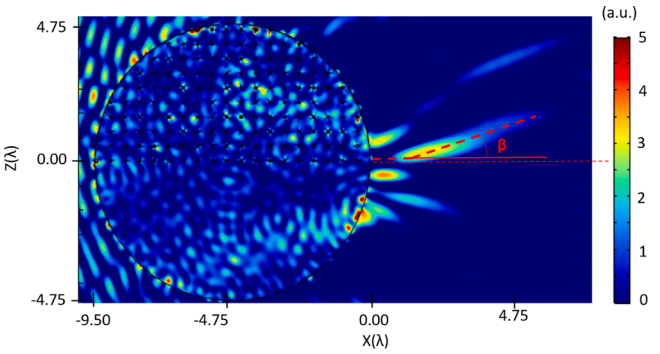

Fig. 6. Angle β to quantify the curvature of the acoustic hook.

Table 2
Numerical parameter results of the bending angle for a 4,75 λ radius Janus cylinder consisting on Rexolite® and SC with 3 mm of lattice constant and different radii, r.

r (mm)	ff (%)	I_{max}/I_{inc}	FWHM/λ	β (°)
0.10	0.35	3.06	0.68	0.00
0.15	0.79	3.88	0.58	0.05
0.20	1.40	4.06	0.59	3.75
0.25	2.18	3.06	0.72	5.82
0.30	3.14	3.38	0.74	12.09
0.35	4.28	2.88	0.88	14.12
0.40	5.59	1.79	1.03	19.18

filled with water. In a such way, we had the lower-half Rexolite® cylinder with a refractive index n_{REX} and the upper-half cylinder with a refractive index n_{SC}. In this work, we took water refractive index as reference, n_W. The refractive index of the upper-half cylinder containing the SC is given by $n_{SC} = ff \cdot n_W + (1 - ff) \cdot n_{REX}$, where ff is the filling fraction, that is the relation between the area occupied by the holes and the area of the lattice.

It is well known that for a SC, the refraction index depends on the ff. In a SC, this parameter depends on the lattice constant, a, (which determines how much the holes are separated from one another) and the size of the hole, which in our case, being cylinders, depends on the radii, r (see Fig. 2). To study the ff influence on the creation of the acoustic hook, we chose a SC with a square lattice and a constant lattice a = 3 mm. The radii of the holes vary from 0.1 mm to 0.4 mm. Fig. 5 shows the distribution of the acoustic intensity I_{max}/I_{inc} in XZ planes around and inside the Janus cylinder with a radius R equal to 4.75λ and with a SC with a = 3 mm and different hole radii on the upper-half cylinder.

Table 3
Numerical parameter results of the bending angle for a 4,75 λ radius Janus cylinder consisting on Rexolite® and SC with 0.3 mm hole radii and different lattice constant.

a (mm)	Ff (%)	I_{max}/I_{inc}	FWHM/λ	β (°)
2	7.07	1.99	0.64	21.12
3	3.14	3.38	0.74	12.09
4	1.77	3.98	0.71	4.66
5	1.13	4.07	0.64	3.06
6	0.79	4.57	0.63	2.63
7	0.58	5.37	0.58	2.98

It is observed that the acoustic hook appears when hole radii increase (equivalently increase the ff) while the lattice constant is fixed. As ff increases, the bending becomes more apparent, although the acoustic intensity of the acoustic hook decreases. To quantify the curvature of the acoustic hook [5,8], this is determined by a midline aided by an angle β between the two lines, which link the start point with the inflection point and the inflection point with the end point, respectively (see Fig. 6). Table 2 shows the numerical results.

The difference in acoustic properties between two half-cylinders results in the breaking of the symmetry in the cylinder. This gives rise to waves passing through each of the cylinder halves with different propagation speeds. Equivalently, using different refractive indices gives rise to a redistribution of the acoustic pressure within and near its shadow surface. The beam outside the cylinder is an interference from the wave fields coming from each of the two halves of the cylinder. Hence, depending on the contrast between the refractive indices of each of the cylinder halves, the bending of the beam and its intensity can vary substantially since the acoustic hook is the result of constructive interference.

In the case of keeping the radii of the holes constant and varying the lattice constant, the results obtained are the same as the previous case. Table 3 shows the numerical results obtained for the case of hole radii, r, constant and equal to 0.3 mm and lattice constant variable from 2 to 7 mm.

We studied the influence that the refractive index contrast between the lower-half and the upper-half cylinder has on the bending angle, β.

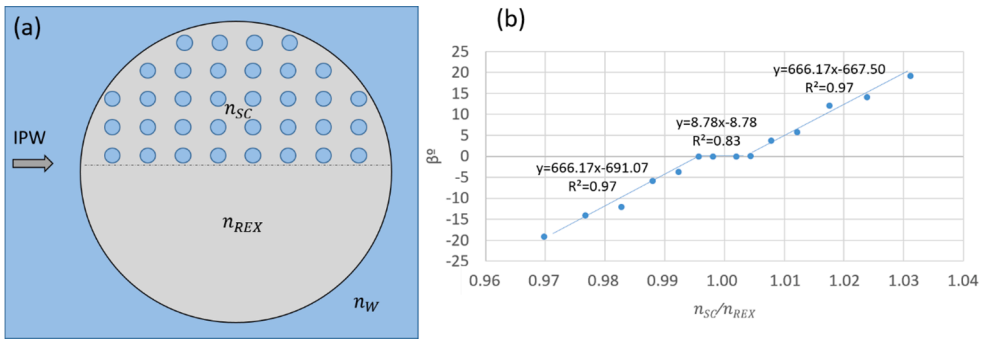

Fig. 7. (a) Schematic view of cylinder, (b) Bending angle β as a function of the refractive index contrast between the lower-half and the upper-half cylinder n_{SC}/n_{REX}.

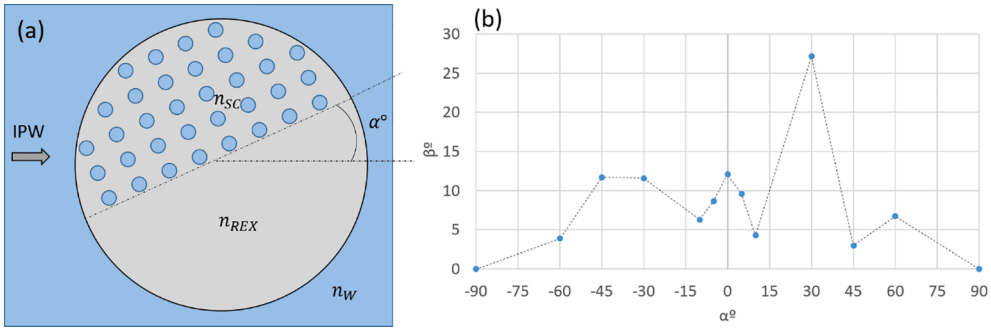

Fig. 8. (a) Schematic view of rotation angle α, (b) Bending angle β as a function of rotation angle α, for a 4,75 λ radius Janus cylinder consisting on Rexolite® and SC with 3 mm of lattice constant and 0.3 mm holes radii.

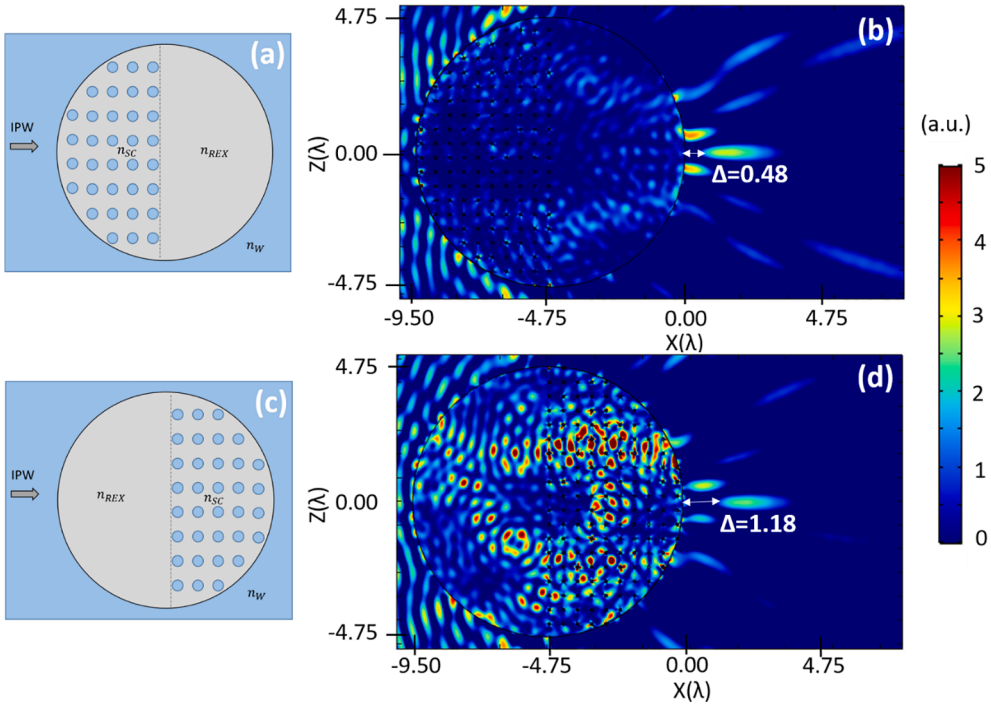

Fig. 9. (a) Schematic view of rotation angle α = 90° and (b) simulation result, where Δ = 0.48λ (c) Schematic view of rotation angle α = −90° and (d) simulation result, where Δ = 1.18λ.

The refractive indices of the two cylinder halves are respectively n_{SC} and n_{REX}, and n_W is the refractive index of water, as shown in Fig. 7(a) When $n_{SC}/n_{REX} > 1$, the bending angle β is positive, while for values of $n_{SC}/n_{REX} < 1$, the bending angle takes negative values, as shown in Fig. 7(b). This shows that the bending angle and the direction of the beam depend on the contrast of refractive indices between the lower-half and the upper-half cylinder. As can be seen in the Fig. 7(b), it is verified that the variation of the angle β with respect to the n_{SC}/n_{REX} ratio is identical both for the case of being greater or less than unity, presenting a linear behavior.

The bending angle can also be tuned by rotating the cylinder a certain angle, either clockwise or counter-clockwise. We call the rotation angle of the cylinder, α, as shown in Fig. 8(a). A 4.75 λ radius Janus cylinder consisting of Rexolite® and a SC with 3 mm lattice constant and 0.3 mm hole radii was analyzed. A rotation angle from −90° to 90° has considered. As can be seen from Fig. 8(b), the maximum bending angle (β = 27.14°) is obtained for a rotation angle, α, of 30°. In this case, the bending angles are always positive, regardless of whether the rotation angle is clockwise or counterclockwise. Therefore, the value of the bending angle does depend on whether the rotation angle is clockwise or counterclockwise. This is due to a redistribution of the acoustic pressure within and near its shadow surface, as discussed above.

The rotation for a 4,75 λ radius Janus cylinder consisting on Rexolite® and a SC with 3 mm of lattice constant and 0.3 mm hole radii is analyzed below. In the case of a rotation angle, α, of 90°, both counterclockwise and clockwise, the bending angle β is 0°. However, in the case of α = -90°, the beam is further from the cylinder than in the case of α = 90°, as shown in Fig. 9. It is observed that the intensity in the focus is greater when −90° has been turned (counter-clockwise) and therefore the SC is on the right side of the cylinder.

Conclusions

The creation of acoustic hooks from Janus cylinder were studied numerically. To obtain the Janus cylinders a Rexolite® cylinder were used. One of the halves was drilled to include sonic crystals. Accordingly, both half-cylinders had different refractive index. Simulation results carried out with the Finite Element Method shown that it was possible to obtain an acoustic hook with an FWHM close to the diffraction limit. Acoustic hooks could be obtained modifying the contrast of the refractive indices of the two half-cylinders or by rotating the Janus cylinder. Results obtained in this paper may have potential applications in the development of new ultrasonic devices for applications in manipulating or trapping objects as well as in the development of instrumentation with medical applications.

CRediT authorship contribution statement

Sergio Castiñeira-Ibañez: Conceptualization, Investigation, Formal analysis, Writing - original draft, Writing - review & editing. **Daniel Tarrazó-Serrano:** Conceptualization, Investigation, Formal analysis, Writing - original draft, Writing - review & editing. **Antonio Uris:** Conceptualization, Investigation, Formal analysis, Writing - original draft, Writing - review & editing. **Constanza Rubio:** Conceptualization, Investigation, Formal analysis, Writing - original draft, Writing - review & editing, Supervision, Project administration, Funding acquisition.

Declaration of Competing Interest

The authors declare that they have no known competing financial interests or personal relationships that could have appeared to influence the work reported in this paper.

Acknowledgement

This work has been supported by Spanish Ministry of Science, Innovation and Universities (grant No. RTI2018-100792-B-I00). D.T.-S. acknowledges financial support from Ministerio de Ciencia, Innovación y Universidades de España through grant BES-2016-077133.

References

[1] Siviloglou GA, Broky J, Dogariu A, Christodoulides DN. Observation of accelerating airy beams. Phys Rev Lett 2007;99:213901.
[2] Siviloglou GA, Christodoulides DN. Accelerating finite energy airy beams. Opt Lett 2007;32:979.
[3] Berry MV, Balazs NL. Nonspreading wave packets. Am J Phys 1979;47:264.
[4] Efremidis NK, Chen Z, Segev M, Christodoulides DN. Airy beams and accelerating waves: an overview of recent advances. Optica 2019;6(5):686–701.
[5] Yue L, Minin OV, Wang Z, Monks JN, Shalin AS, Minin IV. Photonic hook: a new curved light beam. Opt Lett 2018;43(4):771–4.
[6] Minin IV, Minin OV, Katyba GM, Chernomyrdin NV, Kurlov VN, Zaytsev KI, et al. Experimental observation of a photonic hook. Appl Phys Lett 2019;114:031105.
[7] Minin IV, Minin OV, Ponomarev DS, Glinskiy IA. Photonic hook plasmons: a new curved surface wave. Ann Phys 2018;530(12):1800359.
[8] Rubio C, Tarrazó-Serrano D, Minin OV, Uris A, Minin IV. Acoustical hooks: a new subwavelength self-bending beam. Results Phys 2020;16:102921.
[9] Gu G, Shao L, Song J, Qu J, Zheng K, Shen X, et al. Photonic hooks from Janus microcylinders. Opt Express 2019;27:37771–80.
[10] Geints YE, Minin IV, Minin OV. Tailoring 'photonic hook' from Janus dielectric microbar. J Opt 2020;22:065606.
[11] Lopes JH, Andrade MAB, Leão-Neto JP, Adamowski JC, Minin IV, Silva GT. Focusing acoustic beams with a ball-shaped lens beyond the diffraction limit. Phys. Rev. Applied 2017;8:024013.
[12] Minin IV, Minin OV. Mesoscale acoustical cylindrical superlens. In: Siemens E, Mehtiyev A, Syryamkin V, Yurchenko A, editors. MATEC web of conferences, vol. 155; 2018. p. 01029.
[13] Tarrazó-Serrano D, Rubio C, Minin OV, Uris A, Minin IV. Ultrasonic focusing with mesoscale polymer cuboid. Ultrasonics 2020;106:106143.